SAND 2000-2258C

Electrostatic Discharge/Electrical Overstress Susceptibility in MEMS: A New Failure Mode

Jeremy A. Walraven, Jerry M. Soden, Danelle M. Tanner, Paiboon Tangyunyong, Edward I. Cole Jr., Richard E. Anderson, and Lloyd W. Irwin

Sandia National Laboratories, P.O. Box 5800, MS 1081, Albuquerque, NM 87185-1081, USA
email: jawalra@sandia.gov

ABSTRACT

Electrostatic discharge (ESD) and electrical overstress (EOS) damage of Micro-Electro-Mechanical Systems (MEMS) has been identified as a new failure mode. This failure mode has not been previously recognized or addressed primarily due to the mechanical nature and functionality of these systems, as well as the physical failure signature that resembles stiction. Because many MEMS devices function by electrostatic actuation, the possibility of these devices not only being susceptible to ESD or EOS damage but also having a high probability of suffering catastrophic failure due to ESD or EOS is very real. Results from previous experiments have shown stationary comb fingers adhered to the ground plane on MEMS devices tested in shock, vibration, and benign environments [1, 2]. Using Sandia polysilicon microengines, we have conducted tests to establish and explain the ESD/EOS failure mechanism of MEMS devices. These devices were electronically and optically inspected prior to and after ESD and EOS testing. This paper will address the issues surrounding MEMS susceptibility to ESD and EOS damage as well as describe the experimental method and results found from ESD and EOS testing. The tests were conducted using conventional IC failure analysis and reliability assessment characterization tools. In this paper we will also present a thermal model to accurately depict the heat exchange between an electrostatic comb finger and the ground plane during an ESD event.

Key Words: Electrostatic Discharge (ESD), Electrical Overstress (EOS), Scanning Electron Microscopy, Focused Ion Beam, Atomic Force Microscopy, MEMS

ESD & EOS Testing Review

It is well known that any electronic device or assembly will experience damage at some energy level. Short duration, high voltage transient events are common, including lightning, electromagnetic pulses, and human electrostatic discharges. ESD in manufacturing is generally considered to involve a lower level of energy compared to the energy of events such as lightning (an extreme example of ESD) or the misconnection of a device to a low impedance power supply (a common cause of EOS). Therefore, ESD in manufacturing is commonly considered a subset of the wide range of possible EOS events that can damage devices and assemblies.

Some level of electrostatically-generated charge exists in any manufacturing environment. Voltages produced electrostatically can reach magnitudes that will easily destroy semiconductor devices and even damage passive components, such as resistors, in environments that are dry and have no ESD avoidance procedures. Preventing ESD damage to components involves two approaches: (1) control of the manufacturing environment to suppress electrostatic charge generation and damaging discharge events and (2) modification of the component design to increase the ability to withstand an ESD event. The first approach involves implementing proper ESD handling and work environment procedures such as avoiding the use of charge generating materials, the use of grounded wristbands, anti-static smocks, and air ionizers. The second approach involves modifying components to include protection diodes or other ESD protection circuitry to increase the circuit or MEMS-structure ESD damage threshold [3].

To evaluate the ability of a component to withstand an ESD event, it is common to use ESD testing that attempts to simulate a specific type of transient event. ESD events are complex because they are the result of many controlling factors that vary greatly (parasitic capacitances and inductances, types of materials, how these materials contact each other, etc.). Therefore, the ability to adequately replicate a specific ESD situation can be quite difficult. For all of the simulation methods, controlling the impedances and parasitics of the test environment are critical, due to the large high frequency components in the transient event. Without proper tester design and interconnection to the device being tested, waveform degradation due to inherently mismatched source/termination impedances can cause severe ringing, reflection pulses, and other high frequency effects.

DISCLAIMER

The oldest and most common ESD simulation model is based on measurements of human body discharge voltage waveforms. The discharge waveforms for a number of individuals charged to high voltages have been evaluated, as were their capacitances and resistances in various physical positions with respect to their surroundings. Evaluation of the average parameters resulted in the Human Body Model (HBM): a capacitance of 100 pF with a series resistance of 1500 ohms and a decay time constant of 150 ns [4]. HBM testers will typically have the ability to charge the 100 pF capacitor up to several thousand volts and an appropriately controlled relay to provide single or repeated discharges through the 1500 ohm resistor to the device being tested. These testers may also have the option to use other values of capacitors and resistors to simulate other types of ESD waveforms, such as one referred to as the Machine Model (MM) event. Components are classified according to their HBM ESD damage voltage, regardless of polarity, as illustrated in Table 1 [4]. Figs. 1 & 2 and Table 2 show HBM current calibration waveforms. Due to the high level of handling during packaging, MEMS devices may be at particular risk for this type of ESD event. If proper ESD handling procedures are not implemented, then manufacturers must have an understanding of the effects of HBM voltage transients on their products.

The purpose of ESD testing using the Machine Model is to simulate an ESD event involving a machine with a lower source resistance than a person (HBM ESD event). Damage to components by a machine ESD event is often similar to the damage due to a human ESD event, but equivalent damage usually occurs at a significantly lower electrostatic voltage on the machine. A MM tester has a discharge network consisting of a charged 200 pF capacitor and (nominally) zero ohms of series resistance [5]. As with HBM testing, the actual series resistance and inductance of the MM tester are specified by defining the current waveform. Because of the nominally zero resistance, the MM waveform for a zero ohm load (shorting wire) is significantly different than the HBM waveform. The voltage waveform produced from a MM ESD event will be much faster than one produced for an HBM ESD event. Figs. 3 & 4 are current calibration waveforms for a MM ESD event. MEMS devices fabricated without ESD protection may be very susceptible to machine-based voltage transients. MEMS devices such as optical mirrors [6] or printheads [7] are structurally-isolated structures which may be susceptible to MM ESD events.

Class	Voltage Range
0	< 250
1A	250 to < 500
1B	500 to < 1000
1C	1000 to < 2000
2	2000 to < 4000
3A	4000 to < 8000
3B	> or = 8000

Table 1. HBM ESD component classification [4].

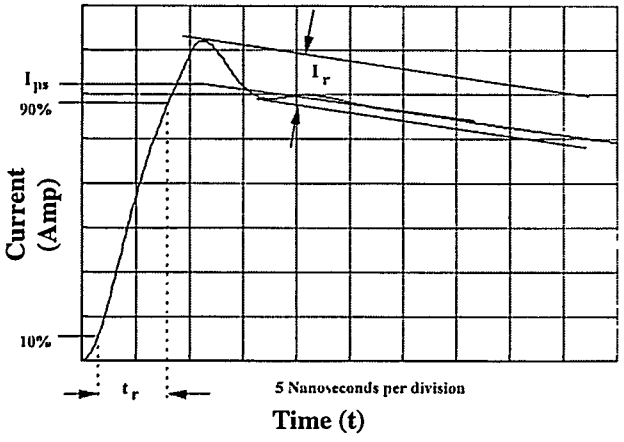

Fig. 1. HBM current waveform through a shorting wire [4].

Parameter	Value
I_{ps} for 250 V stress (amp.)	0.17 (±10%)
I_{ps} for 500 V stress (amp.)	0.33 (±10%)
I_{ps} for 1000 V stress (amp.)	0.67 (±10%)
I_{ps} for 2000 V stress (amp.)	1.33 (±10%)
I_{ps} for 4000 V stress (amp.)	2.67 (±10%)
I_{ps} for 8000 V stress (amp.)	5.33 (±10%)
t_r (pulse rise time)	2 to 10 nanoseconds
I_r (peak to peak ringing)	< 15% of I_{ps}. No ringing 100 nanoseconds after start of pulse
t_d (pulse duration)	150 nanosecond ± 20 nanoseconds

Table 2. Parameters for HBM ESD waveform in Fig. 1 [4].

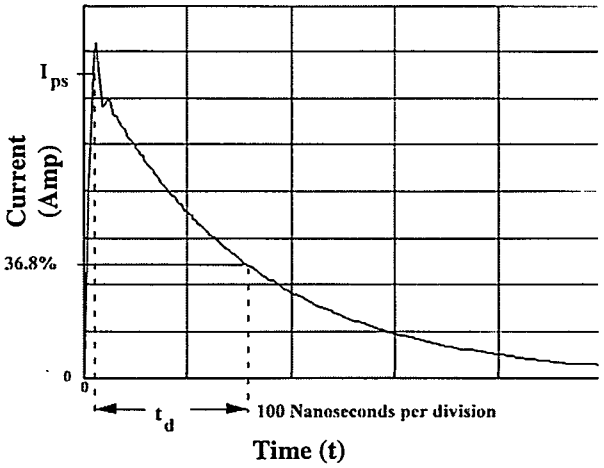

Fig. 2. HBM current waveform through a shorting wire (t_d) [4].

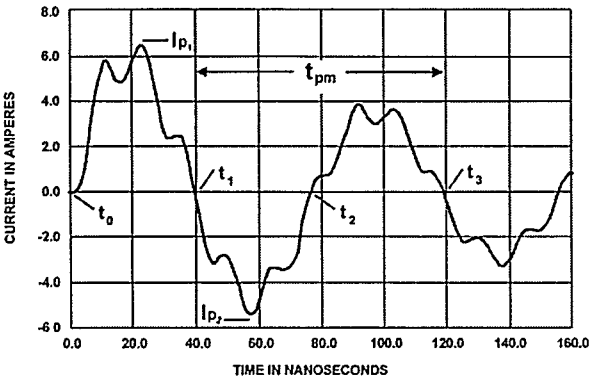

Fig. 3. MM current waveform through a shorting wire for a 400 volt discharge [5].

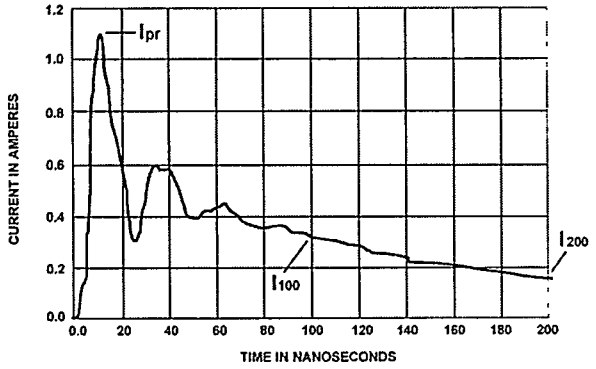

Fig. 4. MM current waveform through a 500 Ω resistor for a 400 volt discharge [5].

Another model of significant interest for ESD testing is based on charging and subsequent discharging of the device itself. A device can be charged by various assembly and testing processes during manufacturing. The method used to simulate this event is referred to as Charged Device Model (CDM) testing. Because the parameters that control the CDM waveform involve the small parasitics of the device and thus the discharge event is faster with correspondingly higher frequency components, the ability to properly simulate this type of event is much more difficult. Standard methods for CDM testing are under development and will be published this year [8]. Charged device damage is more difficult to avoid using device design modifications because the path for charge transfer may not involve the input/output pin circuitry in the same manner as HBM or MM ESD events. The type of damage caused by CDM ESD may be different than the damage produced by HBM or MM ESD. The charge and discharge of a device (or part of a device) that is structurally isolated can possibly cause electrical damage resulting in failure of that component.

BACKGROUND

It has been known for many years that ESD can damage ICs and other semiconductor and electrical devices [9]. This is evident by the extensive development and use of ESD handling procedures and protective circuitry. However, electrostatic and electrical overstress damage in MEMS has not been investigated due to the relative infancy of the field. One model that predicts the breakdown voltage for sub-millimeter gap spacings is Paschen's Law [10]. The "Paschen curve" represents the breakdown voltage between two conductors (V_s) plotted vs the product of the distance between them (d) and the surrounding gas pressure (P, typically ambient atmosphere) $V_s = f(Pd)$ [10]. In the case of electrostatic actuators and other MEMS devices, the small gap spacings "should" prevent a Paschen effect on voltage breakdown due to a lack of ionizing collisions to induce avalanche over a short distance [10]. According to the Paschen curve, smaller gap spacings would lead to higher electrical breakdown fields [10, 11]. However, MEMS devices may have different electrical breakdown behavior due to the geometry of the devices. The Paschen effect is modeled for electrical breakdown between infinitely large parallel plates with no surface topography. But the reality is that polysilicon devices have corners, surface asperities, and other structural features where electric fields may be enhanced. This is not accounted for in the Paschen curve electrical breakdown model. New evidence has shown that the breakdown voltage for small gap spacings in a polysilicon electrostatic actuator is much less than that predicted by the Paschen curve. By not incorporating electric field enhancement, surface roughness, or flexible structures, the Paschen curve may not be a viable model for MEMS structures at small gap spacings. This effect has already been demonstrated for gap spacings ranging from 250 nm to 4 μm in air and vacuum for Al, brass, and Ni [12].

Experimental Approach

ESD

ESD tests were performed using an IMCS Model 2500 ESD tester. This tester was modified for improved HBM waveform characteristics [13-16] with an HBM module (100 pf capacitance). Calibration was performed by a qualified service company [17] as required by the most recent HBM test standard [4] to assure that the waveform met the latest specification requirements and that valid ESD stress data were obtained. The HBM waveform required by this test standard is similar to that of MIL-STD-883D Method 3015.7, but the characteristic and ESD stress test methods are refined to assure optimal HBM ESD event simulation fidelity. The calibration current pulse requirements were shown in Figs. 1 and 2 and Tables 1 and 2. The intent is to create a voltage pulse at the device being tested that has a relatively fast rise time (2 to 5 ns) and slow decay (150 ns). This is sometimes

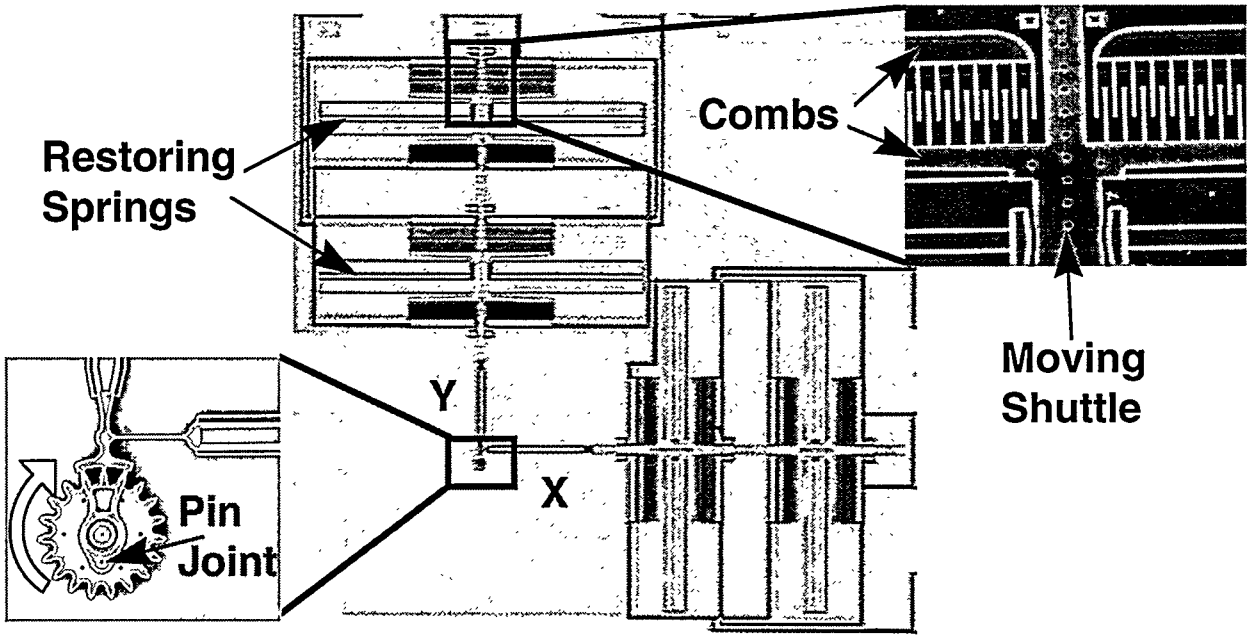

Fig. 5. Sandia microengine with expanded views of the Y comb drive actuator (top right) and the rotating gear (bottom left). The white arrow indicates the direction of gear rotation.

referred to as a double exponential waveform. The IMCS ESD tester and a Tektronix 576 curve tracer were used to test the MEMS device and electrically analyze the part immediately after the ESD pulse.

To assess the affects of an HBM ESD event, Sandia SUMMIT IV MEMS devices, packaged in 24 pin dual in line packages (DIP) containing 4 microengines, were tested. Fig. 5 shows the Sandia microengine consists of orthogonal linear comb drive actuators mechanically connected to a rotating gear. By applying the appropriate drive signals (voltages), the linear displacements of the comb drives are transformed into rotary motion. The X and Y linkage arms are connected to the gear by a pin joint. The gear rotates around a hub, which is anchored to the substrate. Fig. 6 shows the packaged part consisting of one die with four microengines (2 actuators per microengine).

Each microengine is driven by X and Y electrostatic actuators. Each actuator utilizes two drive signals (either up/down or left/right depending upon the orientation of the microengine). These actuators consist of discrete levels of polysilicon to make a two-level comb finger structure. The comb fingers measure 48 μm long and 2 μm wide with a 2 μm space between each comb finger and between the comb fingers and the ground plane. Figs. 7a & b illustrate the comb finger geometry from a front and side perspective.

Prior to ESD testing, each microengine was electrically and structurally characterized to establish electrical continuity and structural integrity. An I-V curve revealing an open circuit would indicate the moveable shuttle (comb fingers) are not in contact with the fixed comb fingers or the ground plane. When the

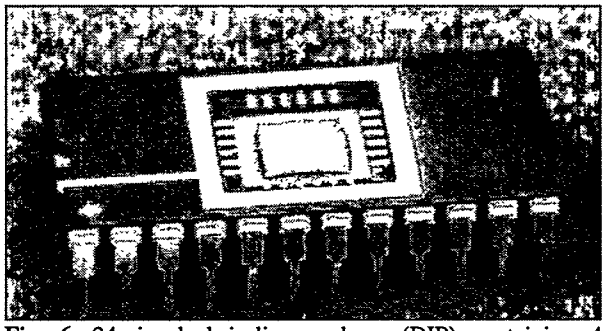

Fig. 6. 24-pin dual in-line package (DIP) containing 4 electrostatically driven microengines (a total of 8 actuators, 16 drive signals).

circuit is electrically shorted, the microengine can not function and the fixed and moveable comb fingers, or a fixed comb finger and the ground plane, are in electrical contact.

Selected actuators were structurally characterized using the scanning electron microscope (SEM) to evaluate the integrity of the comb fingers. This analysis was conducted to determine if contamination or other structural defects were present along the comb fingers prior to the experiment. SEM inspection did not reveal damaged comb fingers, contamination, structural defects, or comb fingers contacting other regions of the microengine. The results from this analysis were compared to the results obtained from the same drive combs after ESD testing to assess for damage or structural degradation. Eleven microengines were tested and 10 were operational, permitting 20 actuators (a sample size of 40 drive signals) for ESD testing.

HBM ESD testing was initiated using a single 100 V pulse. After the 100 V pulse, the voltage was increased

in 10 V increments. The drive signal was electrically characterized after each pulse to verify functionality or identify failure. The drive signal was deemed passing if no shorting events were detected. Prior to each pulse, the drive signal was grounded to remove any residual charge along the comb fingers.

If a drive signal on an actuator was diagnosed as electrically shorted, SEM analysis was used to structurally characterize the actuator. SEM analysis on two-level polysilicon actuators can be difficult due to the complexity of the device, the change in height from the top comb finger to the ground plane, and masking of certain regions by the moveable shuttle. As illustrated in Fig. 7a, the tips of the comb fingers can be analyzed by tilting the device in the SEM. If a shorting event were to occur along the sides of the fixed comb fingers, the moveable shuttle would prohibit characterization (as shown in Fig. 7b).

To aid in analyzing shorted comb fingers, a focused ion beam (FIB) system was employed to excise the moveable shuttle. FIB cuts were performed around the anchored sections of the movable shuttle. Nine FIB cuts were performed, 4 along each anchor (2 anchors) and one along the linkage arm connecting the shuttle to the gear. After the FIB cuts were performed, the movable shuttle was extracted using a probe tip covered with double-stick carbon tape. Fig. 8 depicts the location of the FIB cuts performed along the moveable shuttle to excise it from the device.

SEM characterization after ESD testing revealed the location of the shorted comb finger along each tested comb drive. This process proved to be both arduous and time consuming. After electrical testing was used to determine which drive signal was shorted, the SEM was employed to localize the comb finger causing the short. After localizing the shorted comb finger, SEM analysis revealed significant damage along the ground plane and tips of the comb fingers as illustrated in Figs. 9a & b. The tip of the comb finger is damaged on the bottom side (side adhering to the ground plane). The corner of the comb finger appears to have melted or spot-welded to the ground plane (which has also suffered damage).

The physical damage found after ESD testing

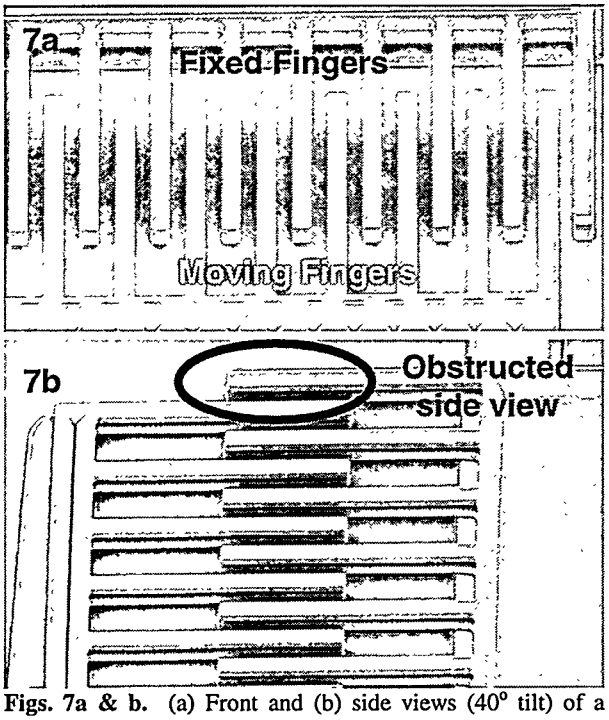

Figs. 7a & b. (a) Front and (b) side views (40° tilt) of a micromachine comb drive actuator. Note that the moveable comb fingers obstruct characterization of the sides of the fixed comb fingers as shown in the black circle at this tilt.

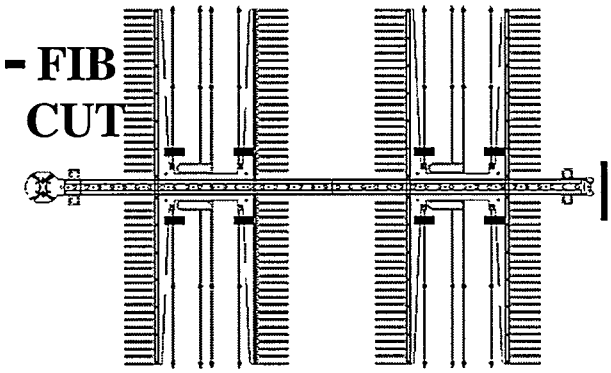

Fig. 8. Autocad rendered image of a Sandia fabricated comb actuator. Each black line represents an area where a FIB cut was performed (4 cuts per spring anchor and 1 cut for the flex arm) [2].

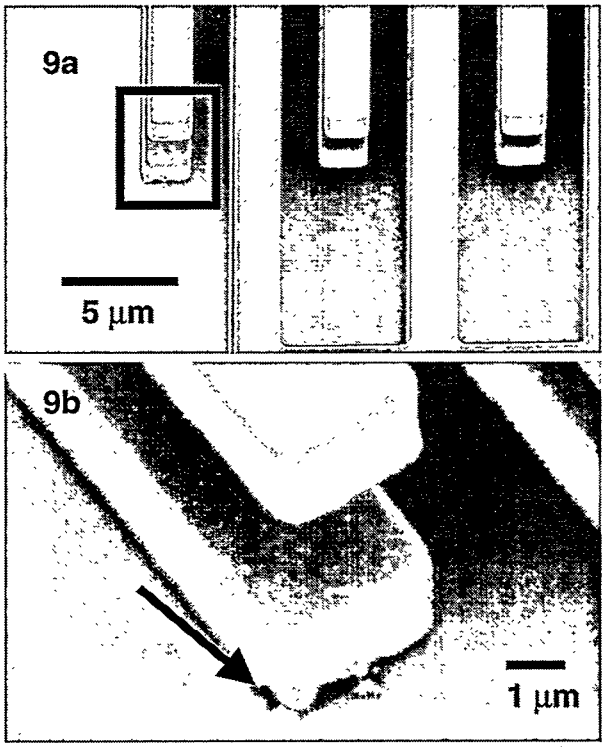

Figs. 9a & b. (a) X-axis actuator, ESD tested up to 150 V revealing a damaged comb finger. (b) Higher magnification revealing melted polysilicon on the edge of the finger and ground plane.

appears to have duplicated the damage found on comb fingers in microengines tested in benign environments [2], vibration [2], and shock [1]. As shown in Figs. 10a & b, a polysilicon comb finger is adhered to the ground plane after a suspected ESD event in a microengine subjected to high levels of vibration without power. The physical signature associated with an ESD event found in polysilicon actuators is the formation of molten silicon along the comb finger and the ground plane (Figs. 9a & b). Figs. 11a & b represent a side profile and a close up of a failed comb finger after a 160 V ESD test. Note the damage along the interface of the comb finger and the ground plane.

In every instance, the shorted comb finger has damage somewhere along the edge of the finger and the ground plane. Since the fingertips are regions where the electric fields are at their highest, it is not surprising that this is the failure site. This physical signature has also been observed on microengines coated with a thin tungsten film [17a], although the damage found on tungsten coated actuators is far more severe than that found on polysilicon actuators.

To identify the power needed to cause polysilicon to melt, thermal modeling was performed to simulate a discharge event between asperities on a comb finger and ground plane [19]. The initial model was closely based on data obtained from an atomic force microscope (AFM). AFM data revealed the surface topography and surface roughness of a poly 1 & 2 laminate comb finger (bottom finger). As illustrated in Fig. 12, the AFM topography image reveals small "nodules" along the surface of the comb finger. The AFM results reveal an RMS surface roughness on the top surface of ~ 7.84 nm.

If one assumes the bottom portion of the comb finger has a similar surface roughness, a thermal model based on an electrical discharge event occurring between comb finger and ground plane asperities can be established. Prior work performed on similar structures indicates that the surface roughness assumption is reasonable. The thermal model illustrated in Fig. 13 simulates the temperature in the asperity areas. The temperature excursion along the asperity peaks is well beyond the melting temperature of polysilicon (1410 °C) [20]. The peak temperature modeled given a 1.35 W event is over 10,000 °C. The power was calculated based upon 10% of a 150V ESD event with a current of 0.09 amp. (13.5 W) passing through a comb finger. Although, this excursion is modeled for a 10 ns discharge event (corresponding to the current peak of an HBM ESD pulse), the temperature is well above the melting temperature for polysilicon.

The electrical discharge may cause more than one comb finger to "weld" to the ground plane. Figs. 14a, b, and c show a failed comb drive from an ESD event. A comb finger is shown contacting the ground plane (Fig. 14b) and another comb finger appears to have contacted the ground plane, but the restoring force in the comb finger caused the comb finger to pop back up (Fig. 14c). It has also been shown that electrostatic comb fingers can recover from an ESD or EOS event.

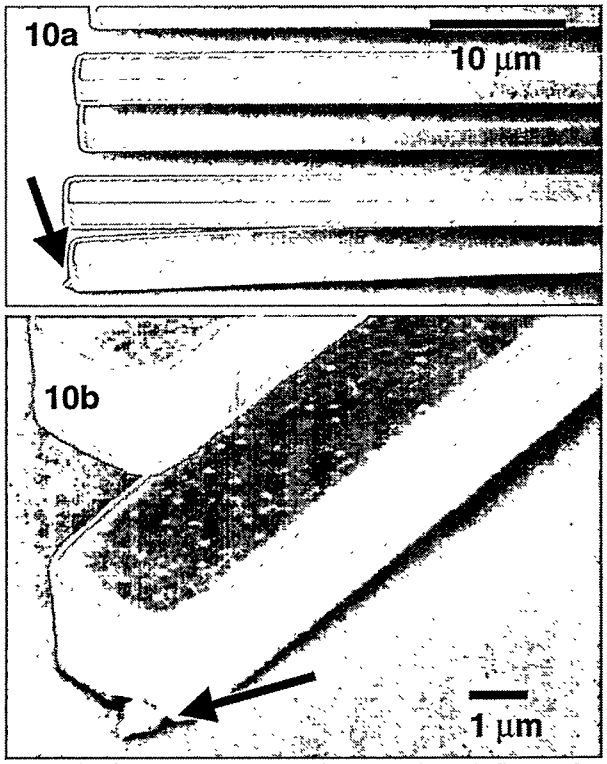

Figs. 10a & b. (a) Side view of a shorted comb finger after high levels of vibration. (b) Damage site present at the tip of the comb finger (arrow) [2].

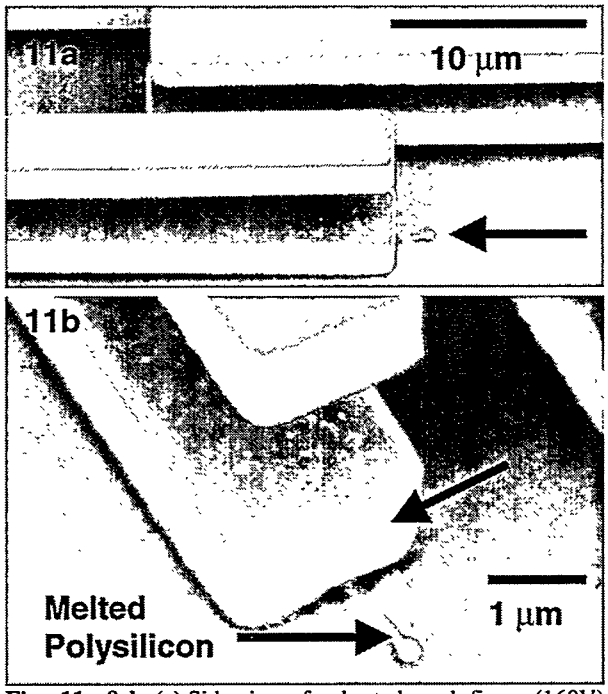

Figs. 11a & b. (a) Side view of a shorted comb finger (160V) with (b) a close up of the adhered region. Note the melted polysilicon droplets (identified with EDX) and damage along the comb finger and ground plane.

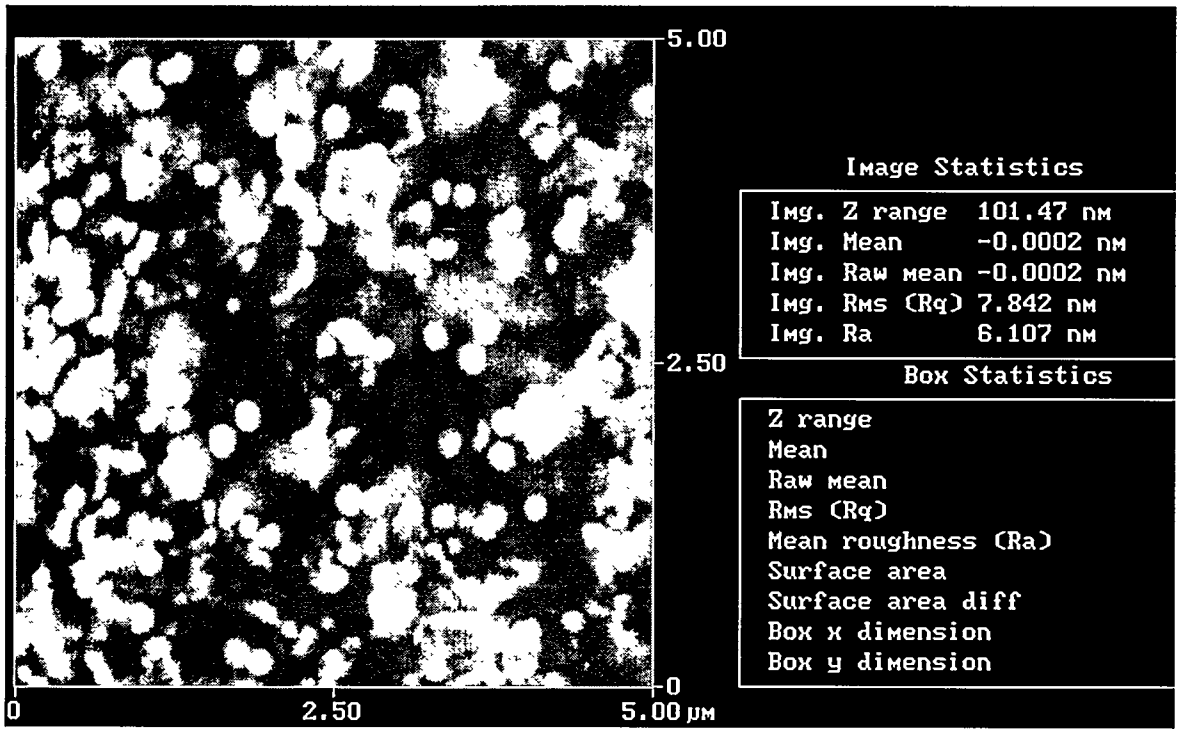

Fig. 12. AFM image of the surface topology along the top surface of a bottom level comb finger. The surface roughness of this comb finger was 7.842 nm.

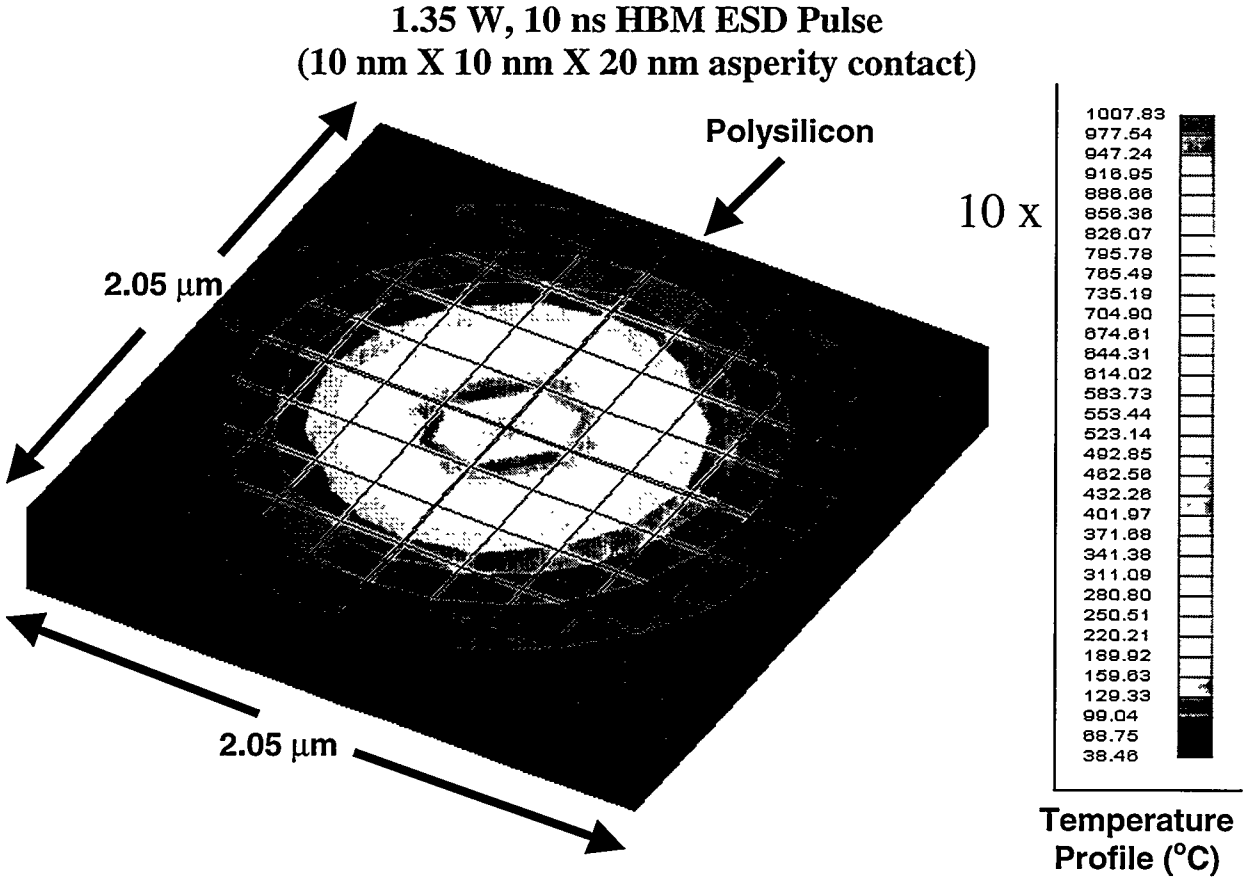

Fig. 13. ESD pulse dissipating 1.35 W through a comb finger asperity (10 nm) to a ground plane asperity (10 nm). The peak discharge time was estimated as 10 ns (based on HBM waveform).

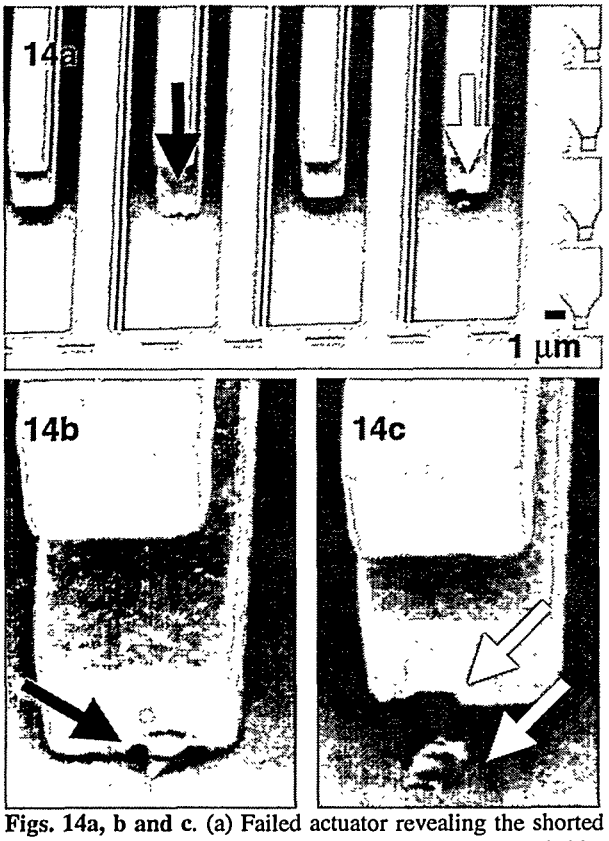

Figs. 14a, b and c. (a) Failed actuator revealing the shorted comb finger (black arrow) and a damaged comb finger (white arrow). (b) and (c) reveal the damage along the comb fingers and ground plane.

The results of ESD testing show that the mean voltage required to produce failure using the HBM testing is ~ 153 V. As shown in Fig. 15, the voltage range found to produce failure of these drive signals ranged from 130 V to 180 V. In every instance, a shorted comb finger occurred along the tested comb drive. In some instances, more than one comb finger was shorted to the ground plane but, in every instance, damage occurred along the ground plane and comb finger.

Using the electrostatic model of Osterberg *et al.* [21] we can calculate the collapse voltage (V_c) required to bring the tip of the comb finger down to the ground plane. The voltage collapse equation is

$$V_c = \sqrt{\frac{8Kg_o^{\ 3}}{27\varepsilon}} \qquad (1)$$

where g_o is the gap between the finger and the ground plane and ε is the permittivity of the gap material. The finger stiffness (K) is defined by

$$K = \frac{2Et^3}{3L^4} \qquad (2)$$

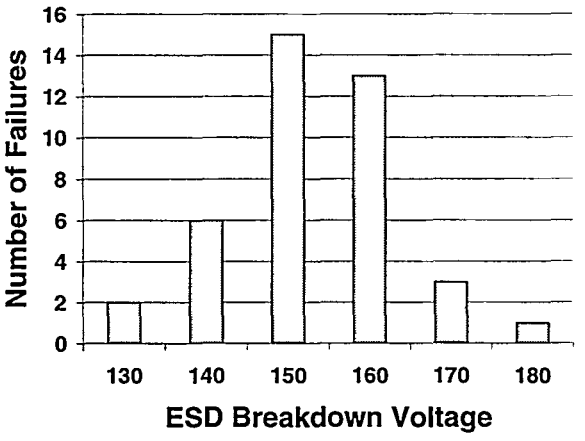

Fig. 15. HBM ESD results of 40 drive signals (20 actuators) tested revealing the voltages required producing failure.

where E is Young's modulus and t and L are the thickness and length of the comb finger. Using a length of 48 μm and thickness of 2.5 μm, a collapse voltage of 285 V is calculated. This is significantly higher than what we measured and this model typically underestimates the collapse voltage because it overestimates the electrostatic force [21]. It is unclear why there is a discrepancy. If we use our measured collapse voltage of 150 V and solve equation (1) for g_o then a gap of 1.3 μm is obtained. This is improbable due to the well-constrained process and low residual stress films [22].

EOS

Electrical overstress testing was performed on seven functional microengines. A Pragmatic Instruments (Model 2414A) waveform generator was used to supply a DC voltage. The voltage was increased in 10 V increments up to 100 V, 5 V increments up to 130 V, and 1 V increments after that. This was to provide fine resolution while approaching 150 V. After each increase in voltage, a continuity check was performed. A failure was recorded at the voltage that the actuator shorted.

Investigation of these failures using the SEM revealed the same signature as the ESD failures. An example is shown in Figs. 16a & b. Note the lower comb finger stuck to the ground plane and the melted polysilicon droplets.

The results of the experiment are shown in Fig. 17. There was a large spread in the data with the average failure voltage being 150 ± 5 V. The spread was primarily caused by the up actuator, which had the lowest EOS breakdown voltage with two failing at 135 V. These low overstress voltages are of concern because they are less than twice the operating voltage of 70 to 90 V, making them susceptible to damage from voltage spikes or other machine modeled transients.

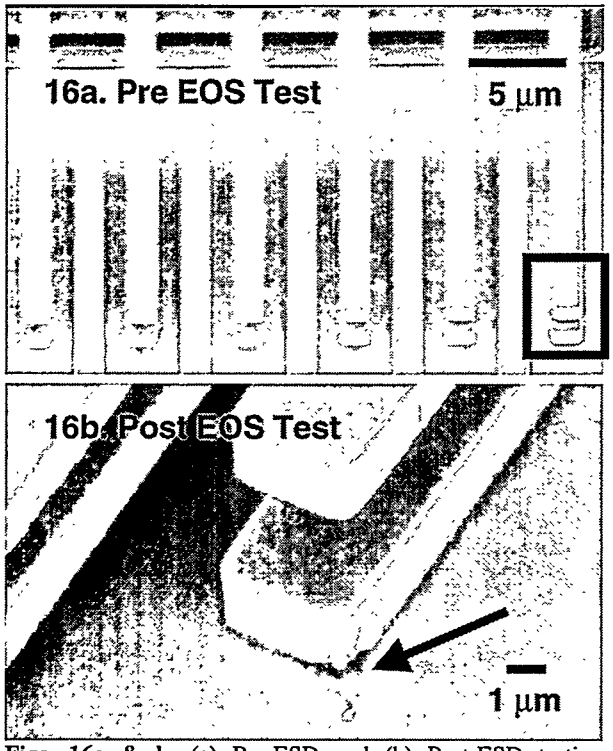

Figs. 16a & b. (a) Pre-ESD and (b) Post-ESD testing revealing a shorted comb finger (boxed region). Note the damage at the end of the fixed comb finger and the ground plane (arrow).

CONCLUSIONS

As shown in polysilicon micromachines, MEMS devices are very susceptible to electrical overstress and electrostatic discharge damage. The reasons may be attributed to enhanced electric field effects surrounding corners of the comb finger(s), asperities producing strong localized electric fields, and the flexiblity of the structures. An electrical short caused by an ESD or EOS event has been shown to "spot weld" a comb finger to the ground plane. The damage found along polysilicon comb fingers appears to be "welding" to the ground plane. New methods are being developed to characterize ESD/EOS and other electrical shorting failure modes quickly and accurately [23].

The evidence presented in this paper suggests MEMS devices are very susceptible to ESD and EOS events at relatively low voltages. This data does not agree with Paschen's Law at small gap spacings, but supports data provided by Torres *et. al.* [12]. This may be due to the flexibility of 48 µm long 2 µm thick polysilicon comb fingers. The mechanism by which the comb fingers fail is not clear. Either the comb finger bends down, contacting the ground plane leading to the electrical short, or if there is electrical breakdown through the 2 µm gap spacing. The evidence does show

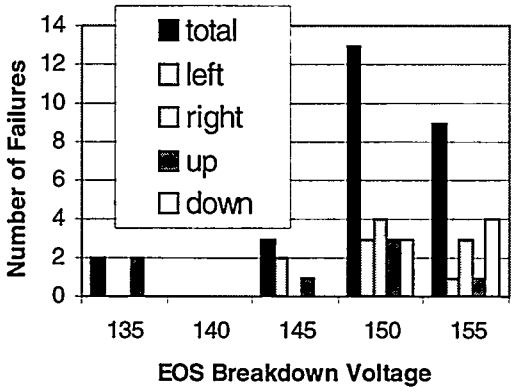

Fig. 17. The distribution of failures from the EOS test. The grouping (left to right) in each bin corresponds to the total failures followed by failures in left, right, up, down.

that the assumptions made in creating the Paschen model can not be accurately applied to micromachines or physical devices with enhanced electric field effects from edges or surface asperities, non-parallel surfaces, flexible components, etc. Enhanced electric field effects from surface asperities and corners causes MEMS devices to not be immune to electrical overstress simply due to small gap spacings.

FUTURE WORK

Further studies testing newly developed MEMS devices for electrical breakdown are pertinent to the growth of MEMS in both government and industrial applications. Addressing the effects of the various ESD models (machine model and charged device model), as well as the effects of cumulative damage will be extremely beneficial towards understanding the effects of an entire system on a device during operation, and the effect of multiple electrical events on the device. Implementing protective measures and examining their effectiveness in improving reliability will also be addressed.

ACKNOWLEDGEMENTS

The authors would like to thank the Sandia microelectronics development laboratory staff for their efforts, Alex Pimentel for his FIB work, and Henry White, Chuck Hembree, and Dan Barton for discussions on ESD sensitivity and prevention. The authors would also like to thank Charles Hembree, Fred Sexton, and Dan Barton for reviewing this paper as well as Kevin Berger of Analytical Solutions Inc., Albuquerque, NM for calibrating and testing our ESD test system. Sandia National Laboratories is a multiprogram laboratory operated by the Sandia Corporation, a Lockheed Martin Company, for the

United States Department of Energy under Contract DE-AC04-94AL85000. For further information about MEMS technology at Sandia, please visit our website at: http:\\www.mems.sandia.gov.

REFERENCES

[1] D. M. Tanner, J. A. Walraven, K. S. Helgesen, L. W. Irwin, F. Brown, N. F. Smith, and N. Masters, "MEMS reliability in shock environments," *Proc. of International Reliability Physics Symposium*, 2000, pp. 129 - 138.

[2] D. M. Tanner, J. A. Walraven, K. S. Helgesen, L. W. Irwin, D. L. Gregory, J. R. Stake, and N. F. Smith, "MEMS reliability in vibration environments," *Proc. Of International Reliability Physics Symposium*, 2000, pp. 139 - 145.

[3] H. Domingos, "Input Protection Design," EOS/ESD Tutorial, Session K, Sept. 1992.

[4] ESD Association Standard Test Method for Electrostatic Discharge (ESD) Sensitivity Testing: Human Body Model (HBM) – Component Level; ESD-STM5.1-1998, February 8, 1998. Waveforms and tables used with permission from the ESD/EOS Association.

[5] ESD Association Standard Test Method for Electrostatic Discharge (ESD) Sensitivity Testing: Machine Model (MM) – Component Level; ESD-STM5.2-1999, May 16, 1999.

[6] S. J. Walker, D. J. Nagel, "Optics & MEMS", Naval Research Laboratories, Materials Science and Technology Division, May 15, 1999.

[7] N. Unal and R. Weschsung, "Inkjet Printheads: An example of MST market reality," *Micromachine Devices*, Vol. 3, No. 1, January 1998, pp. 1-6.

[8] ESD Association Standard Test Method for Electrostatic Discharge Sensitivity Testing: Charged Device Model (CDM) Non-Socketed Mode--Component Level; ESD-DS5.3.1-1996 (Draft Standard).

[9] Proceedings of the EOS/ESD Symposium, 1979-1999 and D.G. Pierce, "Electrostatic Discharge (ESD) Failure Mechanisms," IEEE Int. Reliability Physics Symp., Tutorial Notes, Topic 8, pp. 8.1-8.53, 1995.

[10] F. Paschen, 1889 *Wied. Ann* 37, pp. 69-96.

[11] M. Madou, Fundamentals of Microfabrication, CRC Press, New York, 1997, pp. 58, 59, 412, 413.

[12] J. M. Torres, R. S. Dhariwal, "Electric Field Breakdown at Micrometer Separations in Air and Vacuum," Micro System Technologies 98: 6th International Conference on Micro Electro, Opto, Mechanical Systems and Components, Potsdam, December 1-3, 1998, pp. 295 – 300.

[13] R. G. Chemelli and L. F. DeChiaro, "The Characteristics and Control of Leading Edge Transients from Human Body Model ESD Simulators," Electrical Overstress Electrostatic Discharge (EOS/ESD) Symposium Proceedings, September, 1985, pp. 155-162.

[14] R.G. Chemelli, Personal communications and notes for modications made to his IMCS Model 2400C HBM ESD tester, 1985.

[15] Alliance Analytical, Inc., Report on Evaluation of Sandia's IMCS Model 2500 ESD tester; June 5, 1986.

[16] Alliance Analytical, Inc., Reports on Sandia's IMCS ESD Tester Modification, January 31, 1987 and May 18, 1987.

[17] Analytical Solutions, Inc. (ASI); Albuquerque, NM.

[18] J. A. Walraven, S, S. S. Mani, J. G. Fleming, T. J. Headley, P. G. Kotula, A. A. Pimentel, M. J. Rye, D. M. Tanner, and N. F. Smith, "Failure Analysis of Tungsten Coated Polysilicon Micromachined Microengines," To be published, *Proc. SPIE,* 2000.

[19] Thermal Analysis System, TAS, Harvard Thermal Inc., Harvard MA 01451.

[20] CRC Handbook of Chemistry and Physics, 48th Ed., 1985 - 1986, pp. B34 – B35.

[21] P. Osterburg, H. Yie, X. Cai, J. White, and S. Senturia, "Self-consistent Simulation and Modeling of Electrostatically Deformed Diaphragms," IEEE Proceedings of MEMS 94 conference, 1994, pp. 28-32.

[22] Brian D. Jensen, Maarten P. de Boer, and Sam L. Miller, "IMaP: Interferometry for Material Property Measurement in MEMS," Presented at Modeling and Simulation of Microsystems 1999, San Juan, Puerto Rico, April 19-21, 1999, pp. 206-209.

[23] J. A. Walraven, E. I. Cole Jr., and P. Tangyunyong, "Failure Analysis of MEMS Using Thermally-Induced Voltage Alteration," To be published, International Symposium for Testing and Failure Analysis, 2000.